Supporting Information
Converter domain mutations in myosin alter structural kinetics and motor function

Laura K. Gunther[†1], John A. Rohde[†2], Wanjian Tang[†1], Shane D. Walton[1], William C. Unrath[1], Darshan V. Trivedi[1], Joseph M. Muretta[2], David D. Thomas[2], and Christopher M. Yengo*[1]

[1]Department of Cellular and Molecular Physiology, College of Medicine, Pennsylvania State University, Hershey, PA, 17033

[2]Department of Biochemistry, Biophysics and Molecular Biology, University of Minnesota, Minneapolis, MN 55455, USA

List of Tables and Figures

Table S1. Rate constants used for kinetic simulations of the power stroke, phosphate release, steady-state ATPase, and duty ratio. Kinetic pathway is depicted in Scheme 1 (box) with forward rate constants going from left to right and actin binding/dissociation steps in the M.ATP and M.ADP.Pi stated indicated by $k_{\pm A(ATP)}$ and $k_{\pm A(ADP.Pi)}$, respectively.

Rate/ Eq.Constant	WT	R712G	F750L
[a] $1/K'_{1T}$ (μM)	413	412	383
[a] k'_{+2T} (sec^{-1})	699	661	631
[a] k'_{-2T} (sec^{-1})	≤0.1	≤0.1	≤0.1
[a] $k_{+A(ATP)}$ (sec^{-1})	1000	1000	1000
[a] $k_{-A(ATP)}$ ($\mu M \cdot sec^{-1}$)	10	10	10
[b] k_{+H} (sec^{-1})	195	149	376
[b] k_{-H} (sec^{-1})	96	70	220
[c] $k_{+A(ADP.Pi)}$ ($\mu M \cdot sec^{-1}$)	25-45	25-60	25-45
[c] $k_{-A(ADP.Pi)}$ (sec^{-1})	500	500	500
[d] k'_{+PWF} (sec^{-1})	355	368-450	406
[d] k'_{-PWF} (sec^{-1})	≤0.1	≤0.1	≤0.1
[d] k_{+Pi} (sec^{-1})	1000	1000	1000
[d] k_{-Pi} ($\mu M \cdot sec^{-1}$)	≤0.1	≤0.1	≤0.1
[d] k'_{+PWS} (sec^{-1})	63	121	69
[d] k'_{-PWS} (sec^{-1})	9	11	7
[e] k'_{+ADP} (sec^{-1})	25	25	25
[e] k'_{-ADP} (sec^{-1})	2	2	2
[f] k'_{+ADP} (sec^{-1})	25	25	33
[f] k'_{-ADP} ($\mu M \cdot sec^{-1}$)	≤0.1	≤0.1	≤0.1
Steady-state Parameter	**WT**	**R712G**	**F750L**
k_{cat} $(sec)^{-1}$	8.5	9.1	10.0
K_{ATPase} (μM)	1.4	1.4	1.6
Duty Ratio @ 40μM Actin	0.93	0.91	0.94

[a]Estimated from ATP induced dissociation from pyrene actin (Figure 3)

[b]Calculated from recovery stroke experiment (Figure 5) and mole fractions in the ADP.Pi state (Table 3)

[c]Estimated from reference #27 (Yengo et al, Biochemistry 41, 8508-8517)

[d]Calculated from power stroke experiments (Figure 6) and kinetic simulations

[e]Estimated from simulations of ATPase activity

[f]Calculated from *mant*ADP release experiments (Figure 4B)

<u>Table S2.</u> Transient Time-resolved donor-only fluorescence parameters. Error estimates are ±67% confidence interval determined by error plane analysis.

	Amplitudes		Lifetimes	
Construct	**A_1 (fraction)**	**A_2 (fraction**	**τ_1 (ns)**	**τ_2 (ns)**
WT	0.746 ± 0.015	0.254 ± 0.015	4.716 ± 0.055	1.205 ± 0.039
R712G	0.746 ± 0.015	0.254 ± 0.015	4.716 ± 0.055	1.205 ± 0.039
F750L	*0.647 ± 0.023* ***	*0.353 ± 0.023* ***	4.716 ± 0.055 N.S.; global fit	*1.140 ± 0.011* ***
All parameters were globally fit, except for F750L. This construct affects donor-only fluorescence in a statistically significant manner. For each construct $n \geq 36$. N.S.: $p \geq 0.05$. *: $p < 0.05$. **: $p < 0.01$. ***: $p < 0.001$.				

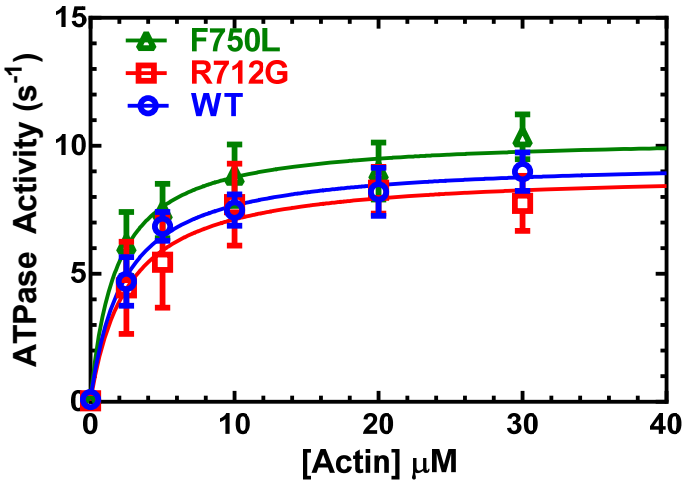

Figure S1. Actin-activated ATPase Activity. The MV converter mutants were compared in the NADH coupled ATPase assay. The average ATPase activity (±SE) is plotted as a function of actin concentration for 4 protein preparations and fit to the Michaelis-Menten relationship. The k_{cat} and K_{ATPase} values for WT, R712G, F750L are summarized in Table 1.

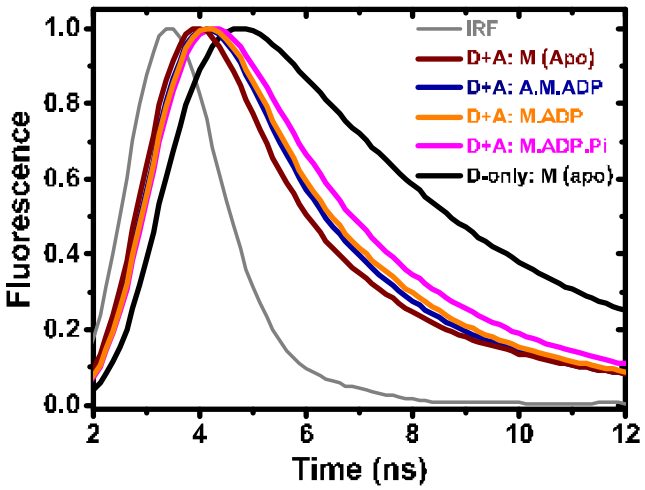

Figure S2. Fluorescence lifetime waveforms under steady-state conditions, detecting time-resolved FRET (TR-FRET). Time-resolved FRET measurements acquired under equilibrium or steady-state ATPase cycling biochemical conditions. The instrument response function (IRF), or detected laser pulse, is shown in gray. Time-resolved fluorescence decays of FRET labeled MV samples (160 nM MV FlAsH.QSY-CaM (Donor + Acceptor, D+A)) in four biochemical states: Apo (maroon), with 20 μM Actin and 4.0 mM ADP (navy), with 4.0 mM ADP (orange), or with 4.0 mM ATP (magenta). The donor-only fluorescence of 160 nM MV FlAsH is shown for comparison (black).

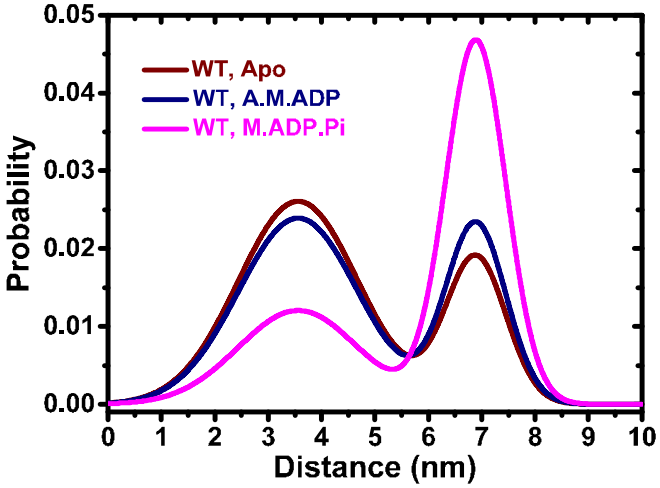

Figure S3. Best-fit two-Gaussian distance distribution model describing TR-FRET between donor and acceptor probes. Interprobe distance distributions in WT MV under Apo (maroon), in the presence of saturating actin and ADP, and under steady-state ATPase cycling conditions (magenta).

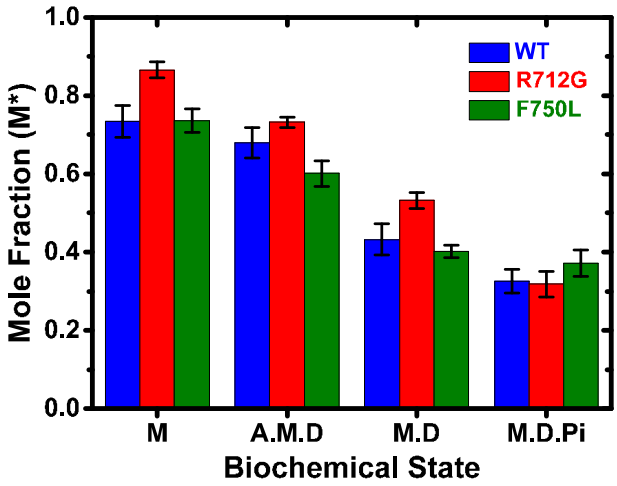

Figure S4. Mole fractions of lever arm orientation in the post-power stroke state. Mole fraction of the post-power stroke state (M*) determined by fitting a two-Gaussian distance distribution model fit to time-resolved waveforms acquired under varied biochemical conditions for wild type MV (WT) or R712G and F750L constructs. Data summarized in Table 3. Error estimates are ±67% confidence interval determined by error plane analysis.

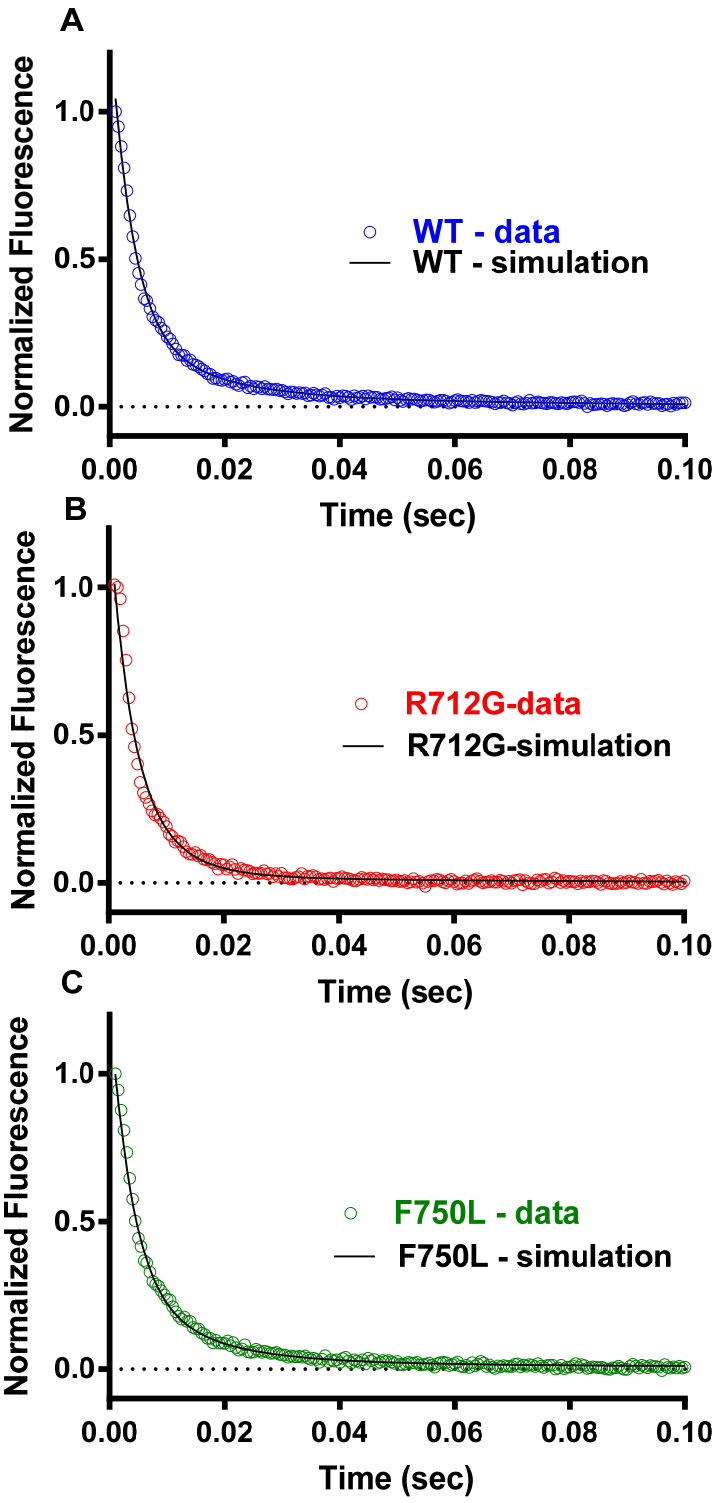

Figure S5. Kinetic simulations of the power stroke. The traces acquired at 40 μM actin were fit to a kinetic model using the rate constants in Table S1. The specific rate constants {(k_{+A} (μM·sec^{-1}), k_{-A} (sec^{-1}), k'_{+PWF} (sec^{-1}), k'_{-PWF} (sec^{-1}), k'_{+Pi} (sec^{-1}), k'_{-Pi} (μM·sec^{-1}), k'_{+PWS} (sec^{-1}), k'_{-PWS} (sec^{-1})} that best fit the WT data were (45, 500, 355, 0.001, 1000,0.001, 63, 9, respectively), and for the R712G data were (45, 500, 368, 0.001, 1000, 0.001, 121,11, respectively), and for the F750L data were (30, 500, 406, 0.001, 1000, 0.001, 69, 7, respectively).

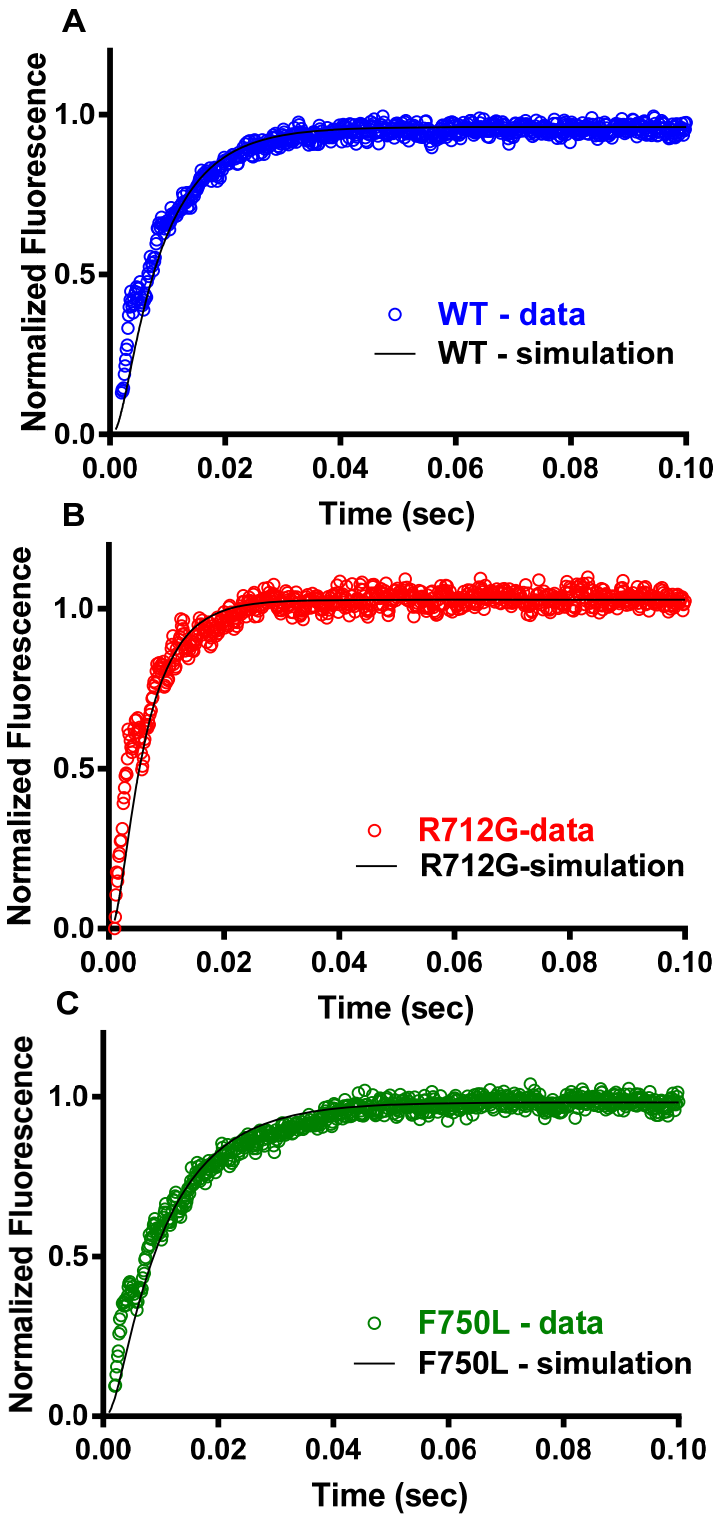

Figure S6. Kinetic simulations of phosphate release. The traces acquired at 10 μM actin were fit to a kinetic model using the rate constants in Table S1. The specific rate constants {(k_{+A} (μM·sec^{-1}), k_{-A} (sec^{-1}), k'_{+PWF} (sec^{-1}), k'_{-PWF} (sec^{-1}), k'_{+Pi} (sec^{-1}), k'_{-Pi} (μM·sec^{-1})} that best fit the WT data were (45, 500, 355, 0.001, 1000, 0.001, respectively), and for the R712G data were (60, 500, 450, 0.001, 1000, 0.001, respectively), and for the F750L data were (30, 500, 406, 0.001, 1000, 0.001, respectively).

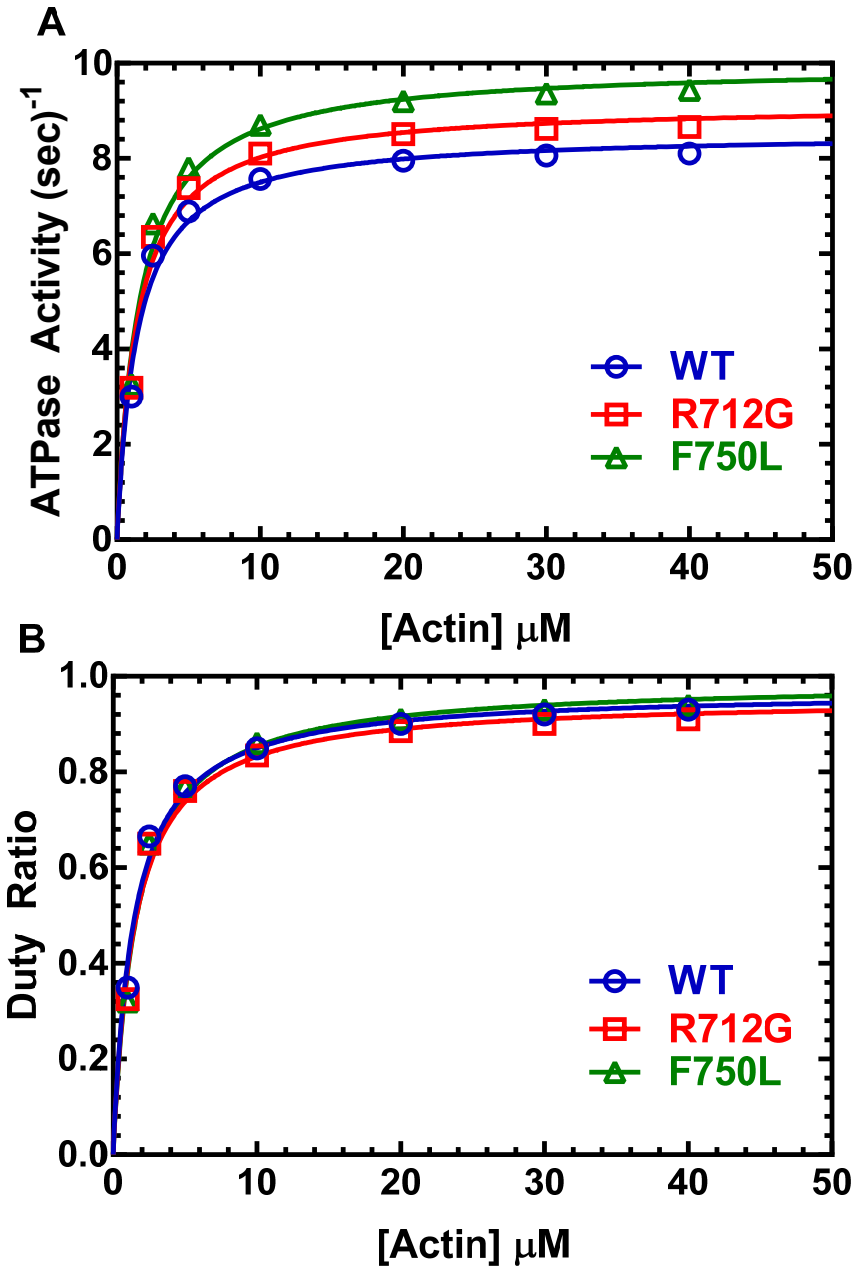

Figure S7. Kinetic simulations of steady-state ATPase Activity and duty ratio. (A) The rate of product formation over time was determined at a series of actin concentrations and fit to the Michaelis-Menten equation to determine k_{cat} and K_{ATPase}. (B) The duty ratio was determined by finding the steady state population of each of the intermediates in the ATPase cycle and plotting the fraction of the actin-attached states as a function of actin concentration. The rate constants used for the simulations were as given in Table S1, except that k_{+A} ($\mu M \cdot sec^{-1}$) = 25 for WT, R712G, and F750L; and k'_{+PWF} (sec^{-1}) = 368 for R712G.

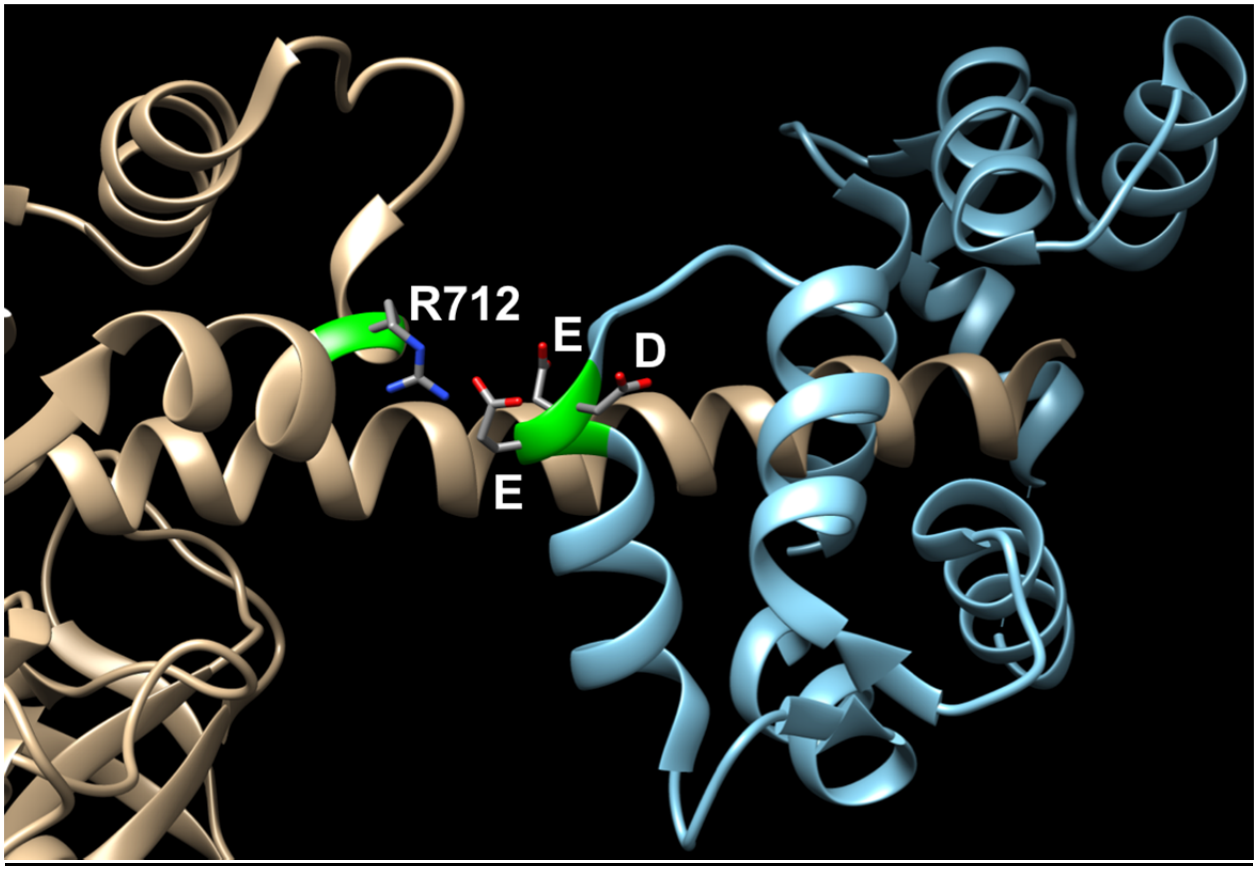

Figure S8. Close-up of the potential interactions between R712 and negatively charged amino acids of the essential light chain. The crystal structure of myosin V complexed with calmodulin (PDB: 4ZLK) which demonstrates the negatively charged amino acids that could potentially interact with R712 of the converter domain. The calmodulin is highlighted in blue and the myosin heavy chain is shown in brown. The negatively charged amino acids in calmodulin depicted are D118, E119 and E120.